Inclusion and reactivity of main group radicals in the porous framework MIL-53(Al)

N. T. Stephaniuk, E. M. Haskings, A. Arauzo, J. Campo and J. M. Rawson

Supplementary Information

S1. Powder X-ray diffraction Studies

S1.1 Phase purity of $(PhCNSSN)_2$, $(PhCNSeSeN)_2$ and MIL-53(Al)

PXRD profiles for each starting material are shown in Figures S1.1a – S1.1c, along with simulations based on single crystal data. Small changes in peak positions are observed which are attributed to differences in measurement temperature between the room temperature experimental PXRD and computed PXRD patterns based on low temperature single crystal data.

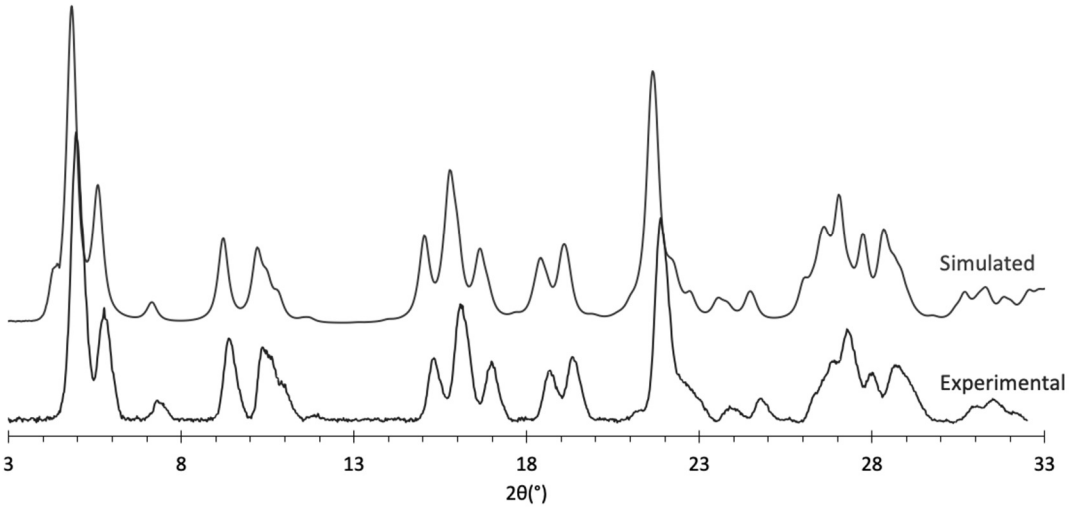

Figure S1.1a Observed room temperature PXRD profile for $(PhCNSSN)_2$ along with the simulated PXRD pattern based on the literature structure (PHTHAZ)

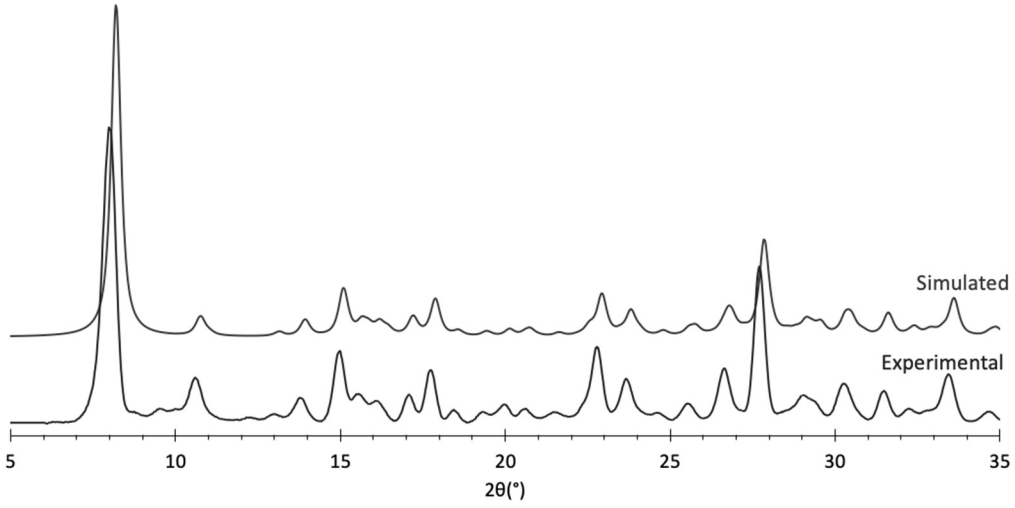

Figure S1.1b Observed room temperature PXRD profile for $(PhCNSeSeN)_2$ along with the simulated PXRD pattern based on the literature structure (JEFBIF)

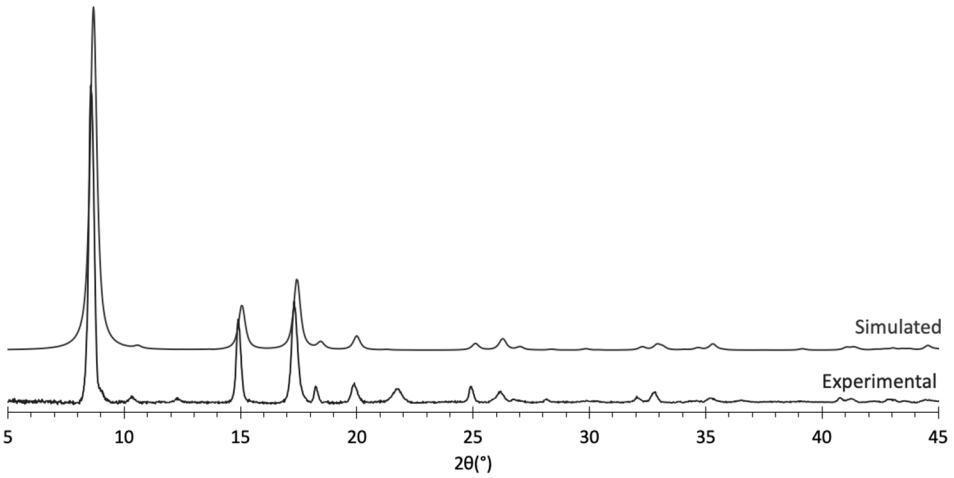

Figure S1.1c Observed room temperature PXRD profile for MIL-53(Al) along with the simulated PXRD pattern based on the literature structure (SABVUN)

S1.2. Synthesis and activation of MIL-53(Al)

Activation of MIL-53(Al) requires emptying the channel structure. The relative intensities of the (0 2 0) reflection around 10^{o} in relation to the (0 1 1) reflection at ca. 8^{o} are diagnostic of activation with the (0 2 0) reflection almost disappearing for activated material (MIL-53(Al)-*ht*) (Figure S1.2).

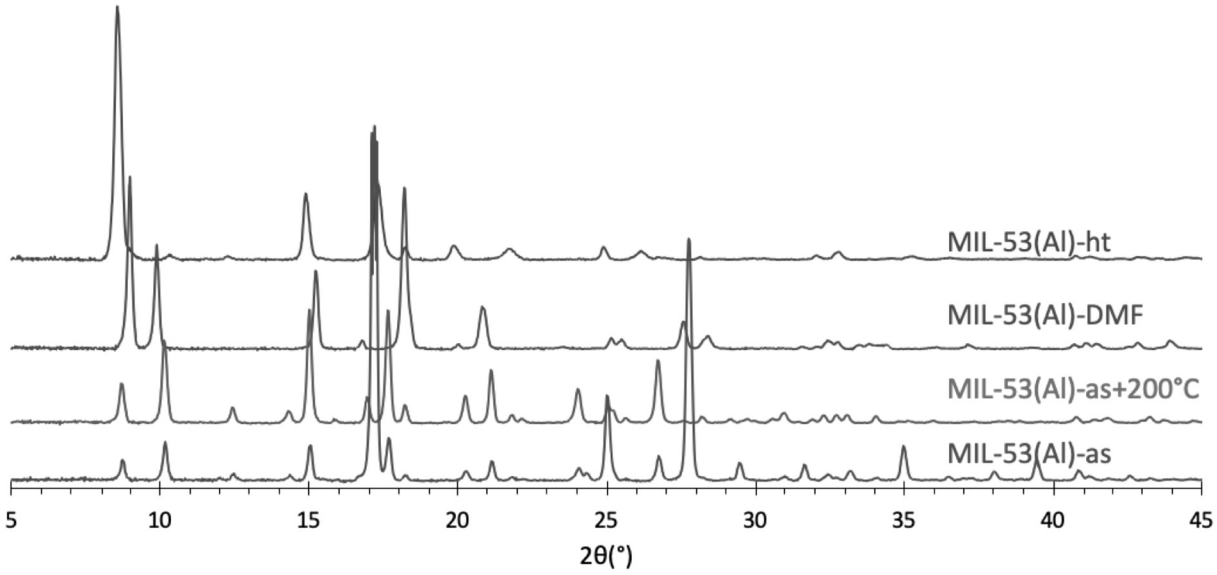

Figure S1.2 PXRD profiles for MIL-53(Al) at different stages during the activation process; MIL-53(Al)-as is the 'as prepared' initial sample of MIL-53(Al); MIL-53(Al)-as+200^{o}C is the 'as prepared' sample, followed by heat treatment at 200 ^{o}C for 4d; MIL-53(Al)-DMF is MIL-53(Al)-as+200^{o}C, followed by microwave heating in DMF at 160 ^{o}C for 1h; MIL-53(Al)-*ht* comprises MIL-53(Al)-DMF followed by heat treatment at 150 ^{o}C for 3d *in vacuo*.

S1.3. Comparison of Commercial and Synthetic MIL-53(Al) PXRD Profiles

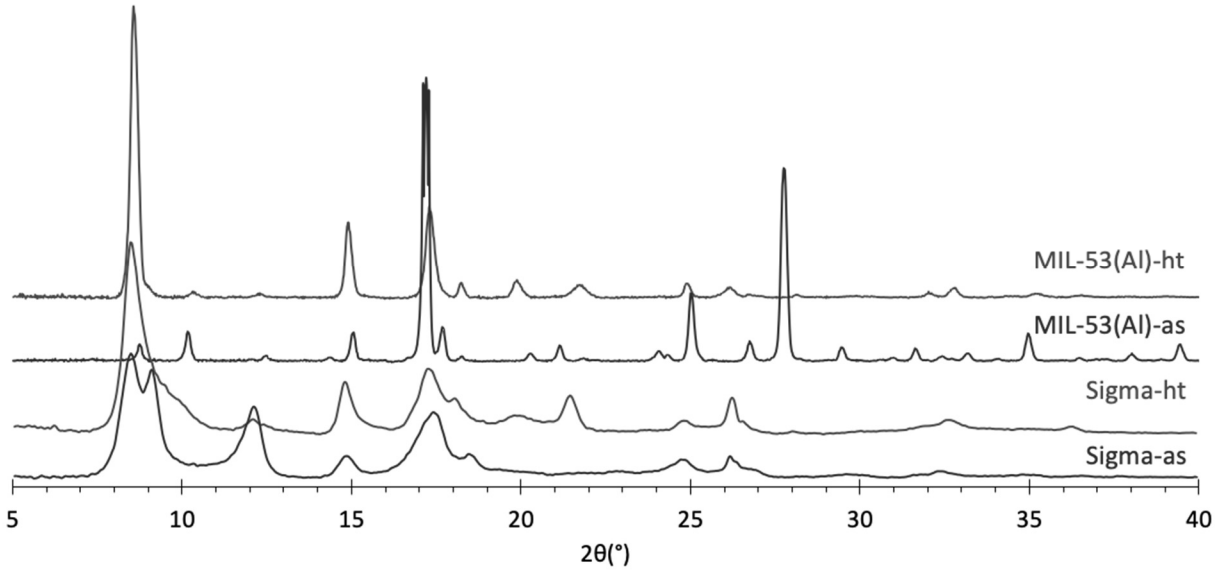

Figure S1.3 Comparison of PXRD profiles for commercial MIL-53(Al) (Sigma), as received (Sigma-as) and after heat treatment (Sigma-ht), alongside MIL-53(Al) as synthesized 'in house' using the microwave method (MIL-53(Al)-as, see experimental) and after activation (MIL-53(Al)-*ht*).

S1.4. Comparison of PhCNSSN@MIL-53(Al) with MIL-53(Al)

Figure S1.4 provides a comparison of the experimental PXRD profile for PhCNSSN@MIL-53(Al) with that calculated based on the structure solution as well as the parent activated MIL-53(Al) framework. A small number of low intensity impurity peaks are evident, e.g. at ca. 13.5^{o} and discussed in detail elsewhere.

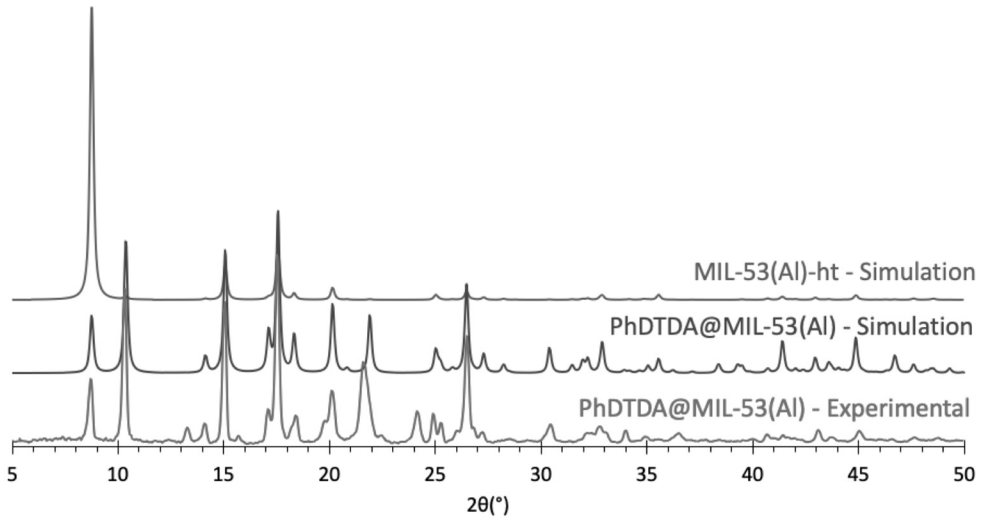

Figure S1.4 Experimental PXRD patterns of PhDTDA@MIL-53(Al) (bottom), compared with the activated framework (MIL-53(Al)-ht, top) and the simulated powder profile for PhCNSSN@MIL-53(Al).

S1.5. Comparison of PhCNSeSeN@MIL-53(Al) with $(PhCNSeSeN)_2$ and MIL-53(Al)

Figure S1.5 provides a comparison of the experimental PXRD profile for PhCNSeSeN@MIL-53(Al), $(PhCNSeSeN)_2$ and the parent activated MIL-53(Al) framework.

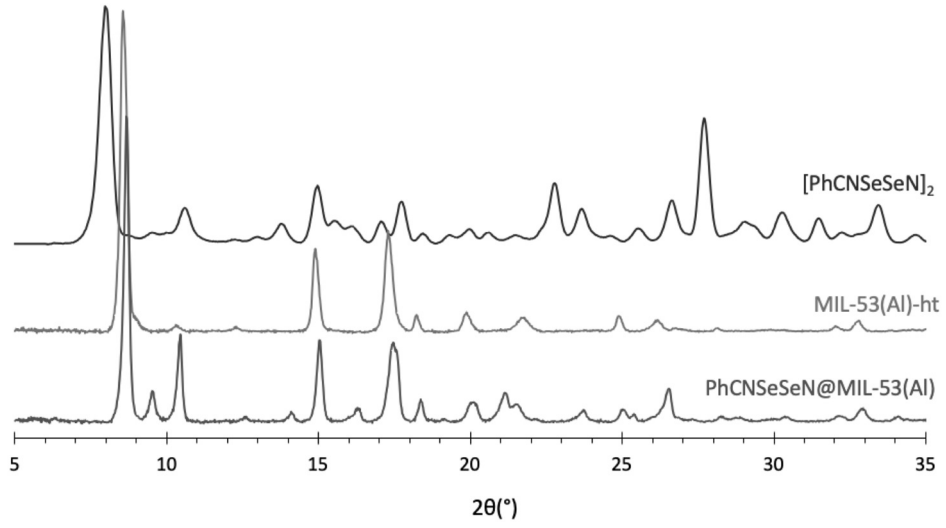

Figure S1.5 Powder X-ray diffraction profiles of $(PhCNSeSeN)_2$ (top), ht-MIL-53(Al) (grey), and the inclusion complex PhCNSeSeN@MIL-53(Al) (purple)

S1.6 Structure determination of PhCNSeSeN@MIL-53(Al) from PXRD data

A comparison of the PXRD profile for PhCNSeSeN@MIL-53(Al) was compared with existing inclusion complexes of MIL-53(Al) and assigned to the orthorhombic Imma setting. A Pawley refinement of the PXRD profile was then undertaken within Expo2014 [A. Altomare, C. Cuocci, C. Giacovazzo, A. Moliterni, R. Rizzi, N. Corriero and A. Falcicchio, *J. Appl. Cryst.*, 2013, **46**, 1231-1235] to extract unit cell parameters. A small number of unindexed reflections were observed but these were of low intensity (Figure S1.6a).

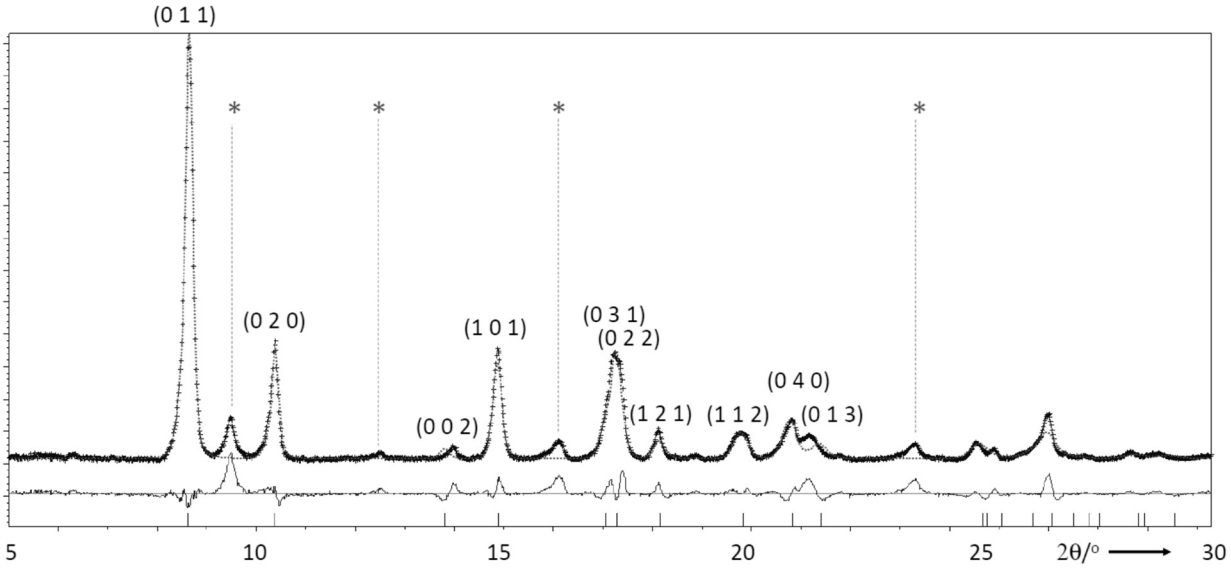

Figure S1.6a Powder pattern for PhCNSeSeN@MIL-53(Al) with Pawley profile fitting (R_p = 16.22, R_{wp} = 24.81). Reflection positions are highlighted with tick marks at the bottom with Miller indices for the low angle reflections assigned. Low intensity impurity peaks not associated with the Imma phase are marked *.

The indexed cell parameters and Pawley fitting parameters are presented in Table S1.6a. In the Imma space group, the asymmetric unit of the host lattice comprises just six non-H atoms with many of these located on special positions. To locate the positions of the framework atoms, the Al was fixed at (0.75, 0.25, 0.75) and a dummy atom ((H atom with sof = 0.01) was implemented at the centroid of the phenylene ring. The positions of the host framework atoms were determined using a simulated annealing process within DASH with the Al to ring-centroid constrained to lie parallel to the (1 1 -1) direction. In this process several of the atoms in the asymmetric unit were located just off their idealized special positions and the 'correct' site was determined by averaging the two sets of symmetry equivalent coordinates which were located either side of the expected symmetry element. Subsequent refinement then used a fixed host framework and a further round of simulated annealing employed a rigid-body refinement with either a monomeric PhCNSeSeN radical (with site occupancy corresponding to 0.20PhCNSeSeN@MIL-53(Al)) or a cis-oid $(PhCNSeSeN)_2$ molecule (with a site occupancy factor equivalent to 0.24PhCNSeSeN:MIL-53(Al)).Both models afforded similar computed diffraction profiles (Figure S1.6b) with the radicals disordered within the channel structure (Figure S1.6c).

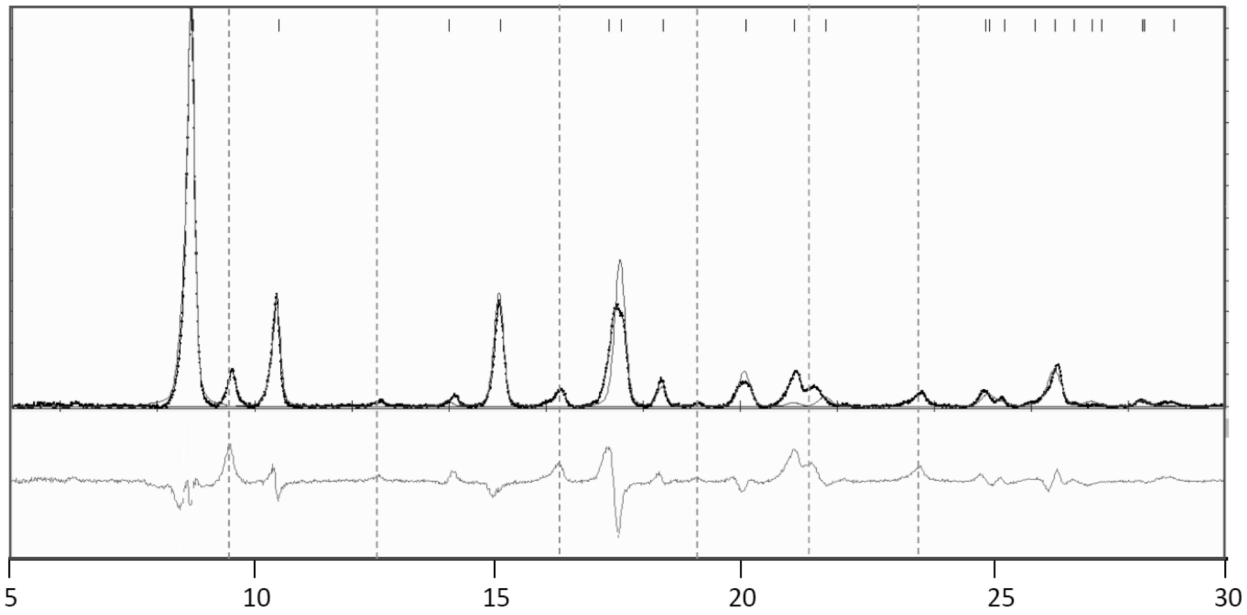

Figure S1.6b Experimental (+) and simulated (---) PXRD pattern for 0.2PhCNSeSeN@MIL-53(Al) with computed difference profile (green). Green dashed lines mark minor reflections arising from the monoclinic phase of MIL-53(Al).

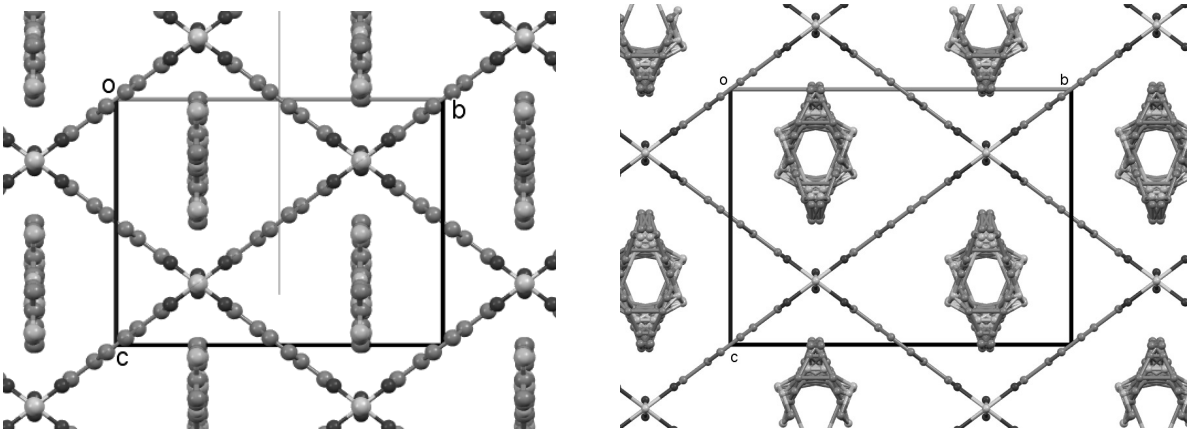

Figure S1.6c Packing of PhCNSeSeN@MIL-53(Al): (left) using a PhCNSeSeN model; (right) using a cis-oid π-dimer, $[PhCNSeSeN]_2$ model

Table S1.6 Unit cell parameters and refinement parameters for PhCNSeSeN@MIL-53(Al)

Temperature	298(2) K	
Radiation	Cu-Kα (1.54056 Å)	
Crystal System	Orthorhombic	
Space Group	Imma	
Unit cell parameters	*a* = 6.6125 Å	α = 90°
	b = 16.7601 Å	β = 90°
	c = 12.5778 Å	γ = 90°
Profile fitting	R_p = 16.22, R_{wp} = 24.81	
	Model 1	Model 2
Chemical Formula	C_8O_5Al, 0.2 $C_7N_2Se_2$	C_8O_5Al, 0.12 $(C_7N_2Se_2)_2$
Final fitting parameters	χ_p^2 = 0.53, χ^2_{int} = 74.22	χ_p^2 = 0.56, χ^2_{int} = 86.65

S1.7 Indexing of PhCNSSN@MIL-53(Al) from PXRD data

A comparison of the PXRD profile for PhCNSSN@MIL-53(Al) was compared with existing inclusion complexes of MIL-53(Al) and assigned to the orthorhombic Imma setting. A Pawley refinement of the PXRD profile was then undertaken within Expo2014 [A. Altomare, C. Cuocci, C. Giacovazzo, A. Moliterni, R. Rizzi, N. Corriero and A. Falcicchio, *J. Appl. Cryst.*, 2013, **46**, 1231-1235] to extract unit cell parameters. This compound also revealed a small number of impurity reflections which were more intense than those observed for PhCNSeSeN@MIL-53(Al) and reflected in the larger R_p and R_{wp} values extracted form fitting of the powder profile. The indexed cell parameters and Pawley fitting parameters are presented in Table S1.7. Structure solution was not attempted in this case due to (i) the likely disorder which was apparent in the structure of PhCNSeSeN@MIL-53(Al) and (ii) overlapping of some impurity peaks with the orthorhombic Imma phase making extracted intensities uncertain.

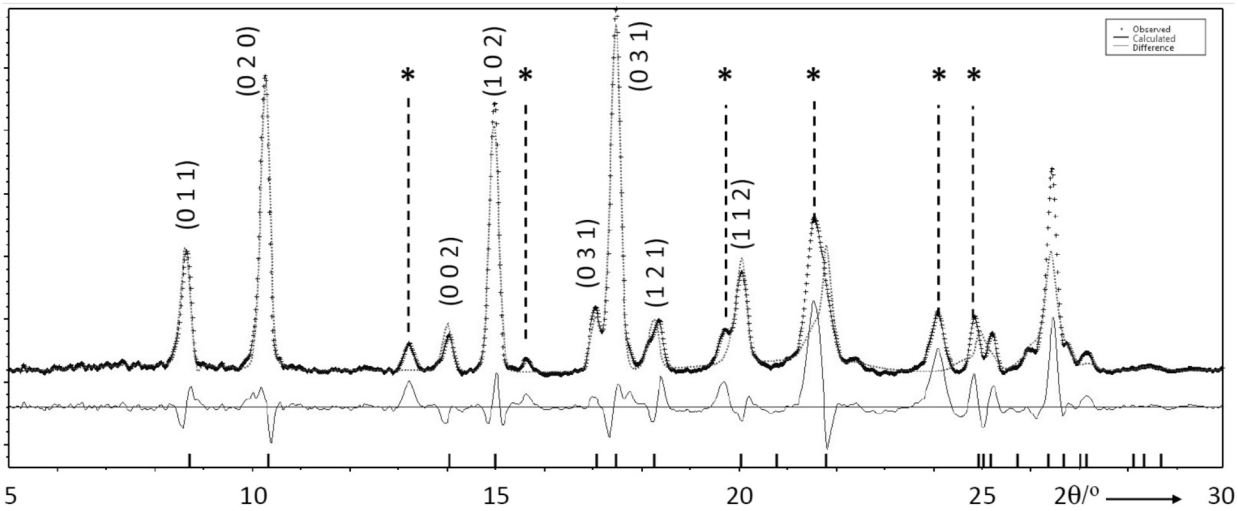

Figure S1.7a PXRD pattern for PhCNSSN@MIL-53(Al) with Pawley fitting of the profile (R_p = 21.14, R_{wp} = 29.18). Reflections not associated with the Imma phase are marked *. Reflection positions for the Imma space group are highlighted with tick marks at the bottom with Miller indices for the low angle reflections assigned.

Table S1.7a Unit cell parameters and refinement parameters for PhCNSSN@MIL-53(Al) from Pawley refinement within the Imma pace group.

Chemical Formula	C_8O_5Al, 0.8 $C_7N_2S_2$	
Temperature	298(2) K	
Radiation	Cu-Kα (1.54056 Å)	
Crystal System	Orthorhombic	
Space Group	Imma	
Unit cell parameters	*a* = 6.6788 Å	$\alpha = 90^o$
	b = 17.0824 Å	$\beta = 90^o$
	c = 12.5935 Å	$\gamma = 90^o$
Profile fitting	R_p = 21.14, R_{wp} = 29.18	

S1.8 Variable temperature PXRD studies on PhCNSSN@MIL-53(Al)

A stack plot of the PXRD profiles for PhCNSSN@MIL-53(Al) from room temperature to 400 ^oC is shown in Figure S1.8. Refined unit cell parameters based on a Pawley refinement of the peak profile at each temperature are summarized in Table S1.8.

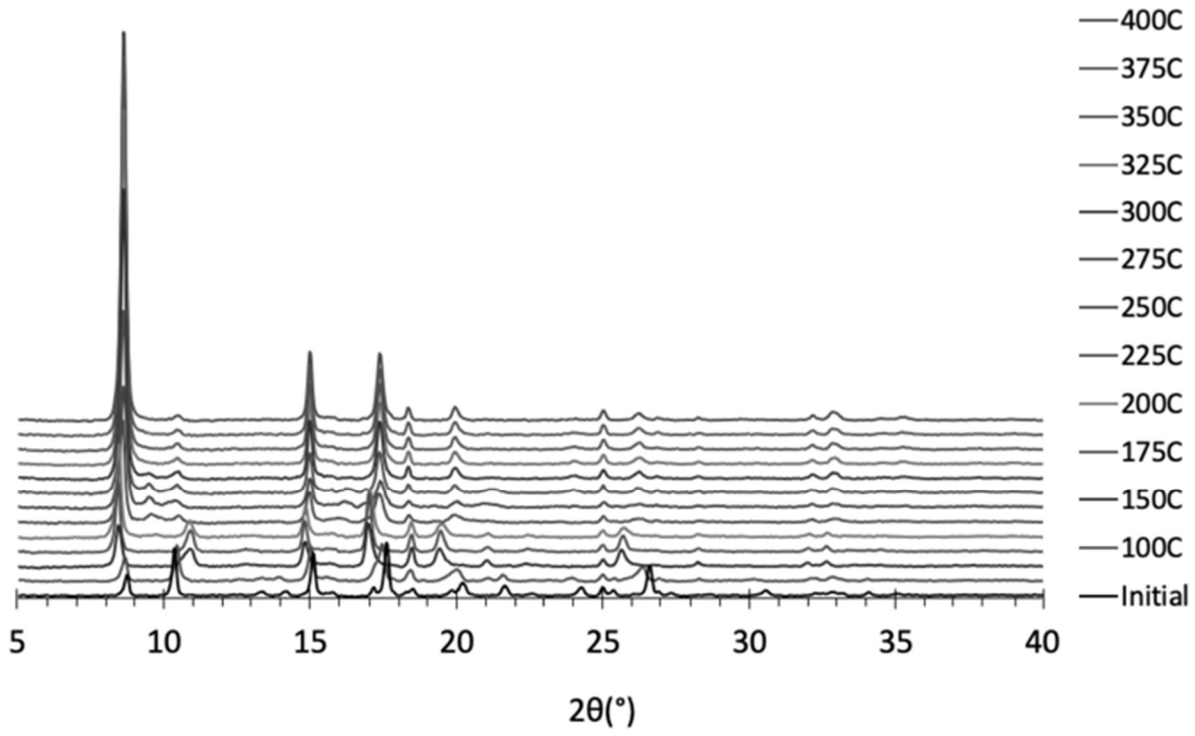

Figure S1.8 Temperature dependence of the PXRD profile of PhCNSSN@MIL-53(Al)

Table S1.8 Unit cell parameters for PhCNSSN@MIL-53(Al) based on the Imma space group, along with the refined profile residuals for temperatures in the range 25 – 250 ^{o}C.

Temp/ ^{o}C	*a*/Å	*b*/Å	*c*/Å	V/ Å^3	χ^2_p
25	6.61292	16.95406	12.44250	1395.0	5.07
100	6.64594	16.88603	12.70797	1426.1	5.12
150	6.62444	16.15305	13.56890	1451.9	2.36
175	6.63760	16.14276	13.62474	1459.9	3.07
200	6.62635	16.19742	13.50586	1449.6	2.37
225	6.62376	16.63339	13.12519	1446.1	2.98
250	6.62386	16.58365	13.04867	1433.4	3.06

S1.9 Variable temperature PXRD studies on PhCNSeSeN@MIL-53(Al)

A stack plot of the PXRD profiles for PhCNSSN@MIL-53(Al) from room temperature to 400 ^{o}C is shown in Figure S1.9. Refined unit cell parameters based on a Pawley refinement of the peak profile at each temperature are summarized in Table S1.9.

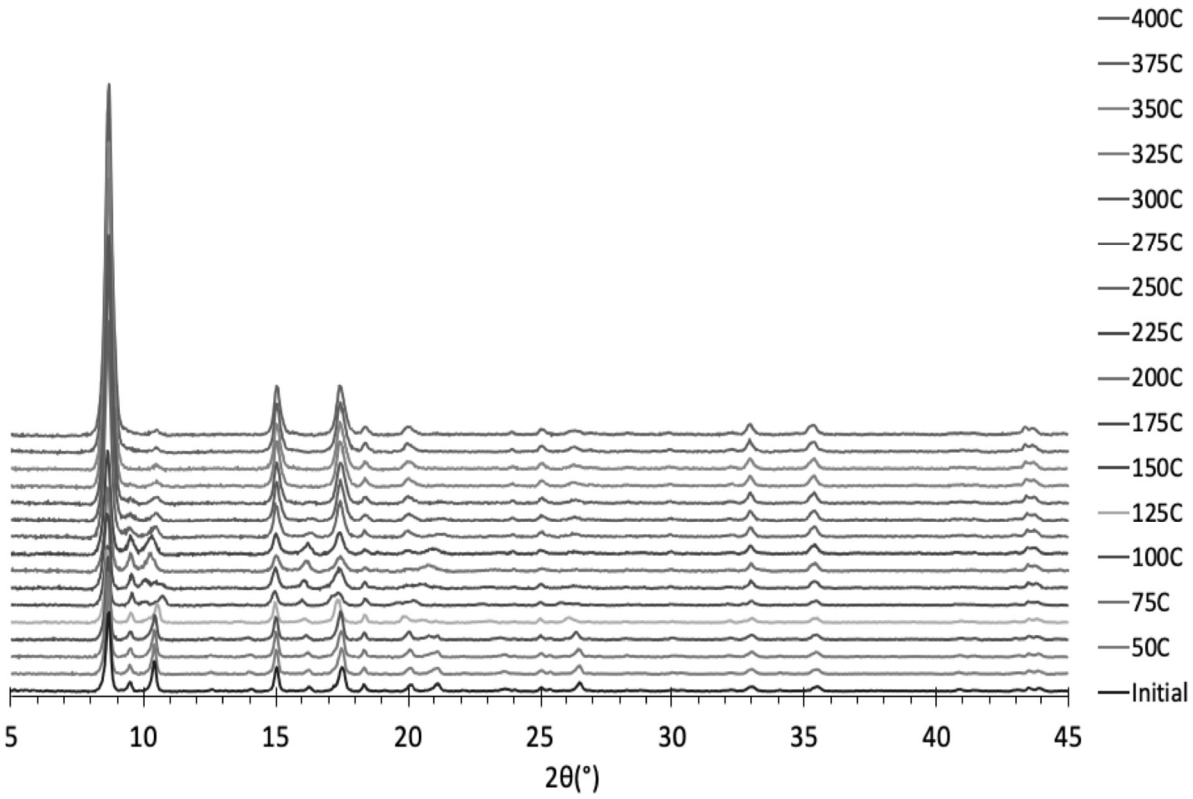

Figure S1.9 Temperature dependence of the PXRD profile of PhCNSeSeN@MIL-53(Al)

Table S1.9 Unit cell parameters for PhCNSeSeN@MIL-53(Al) based on the Imma space group, along with the refined profile residuals for temperatures in the range 25 – 250 °C.

Temp/ °C	*a*/Å	*b*/Å	*c*/Å	V/ Å^3	R_p , R_{wp}
25	6.583176	16.724697	12.494618	1375.7	32.54, 42.71
50	6.568575	16.682714	12.482200	1367.8	32.21, 42.21
75	6.603642	16.765610	12.553396	1389.8	33.28, 41.57
100	6.607687	16.749132	12.598109	1394.3	43.16, 49.35
125	6.606235	16.657215	12.684070	1395.8	47.06, 51.12
150	6.631491	16.617901	12.758493	1406.0	58.49, 56.72
175	6.625915	16.764519	12.633952	1403.4	55.27, 53.75
200	6.618429	16.923599	12.487716	1398.7	56.08, 57.23
225	6.579530	16.718260	12.486811	1373.5	50.49, 52.07
250	6.631390	16.778416	12.648467	1407.3	27.96, 34.70
275	6.649993	16.835020	12.727554	1424.9	22.50, 32.55
300	6.588337	16.673334	12.636983	1388.2	19.43, 28.17

S2. Elemental analysis

S2.1 PhCNSSN@MIL-53(Al)

C and H composition is rather invariant to loading of PhCNSSN in the framework due to the similar C and H content of MIL-53(Al) and PhCNSSN (Table S2.1). Conversely the N content provides a useful measure of radical loading (Table S2.1). Some variation in loading was observed between samples, falling in the range PhCNSSN: MIL-53(Al) = 0.3:1.0 – 0.5:1.0.

Calc	C	H	N
MIL-53(Al)	46.20%	2.42%	0.00%
PhCNSSN	46.41%	2.78%	15.47%
Sample #1			
Found	44.91%	1.55%	3.56%
0.34PhCNSSN@MIL-53(Al)	46.25%	2.51%	3.53%
Sample #2			
Found	45.61%	2.73%	4.93%
0.53PhCNSSN@MIL-53(Al)	46.28%	2.54%	4.89%

Table S2.1 Elemental analysis data for two representative as synthesized samples of PhCNSSN@MIL-53(Al). Sample #1 was implemented for SQUID studies

S2.2 PhCNSeSeN@MIL-53(Al)

Table S2.2 shows compositions based on two representative samples of PhCNSeSeN@MIL-53(Al), reflecting consistency with the extent of radical loading.

Calc	C	H	N
MIL-53(Al)	46.20%	2.42%	0.00%
PhCNSeSeN	30.55%	1.83%	10.19%
Sample #1			
Found	42.46%	2.70%	2.17%
0.20PhCNSeSeN@MIL-53(Al)	42.93%	2.30%	2.13%
Sample #2			
Found	42.39%	2.74%	2.38%
0.23PhCNSeSeN@MIL-53(Al)	42.55%	2.29%	2.29%

Table S2.2 Elemental analysis data for two representative as synthesized samples of PhCNSeSeN@MIL-53(Al). Sample #1 was implemented for SQUID studies

S3. Thermal Studies

S3.1 DSC Studies on PhCNSSN@MIL-53(Al)

DSC studies were undertaken on PhCNSSN@MIL-53(Al) as well as pristine $(PhCNSSN)_2$ and activated MIL-53(Al). The parent radical exhibits a distinct endotherm in the region 110 – 120 ^{o}C (Figure S3.1) but the pristine MIL-53(Al) framework and the PhCNSSN@MIL-53(Al) inclusion complex show no clear exotherm or endotherm in this temperature range.

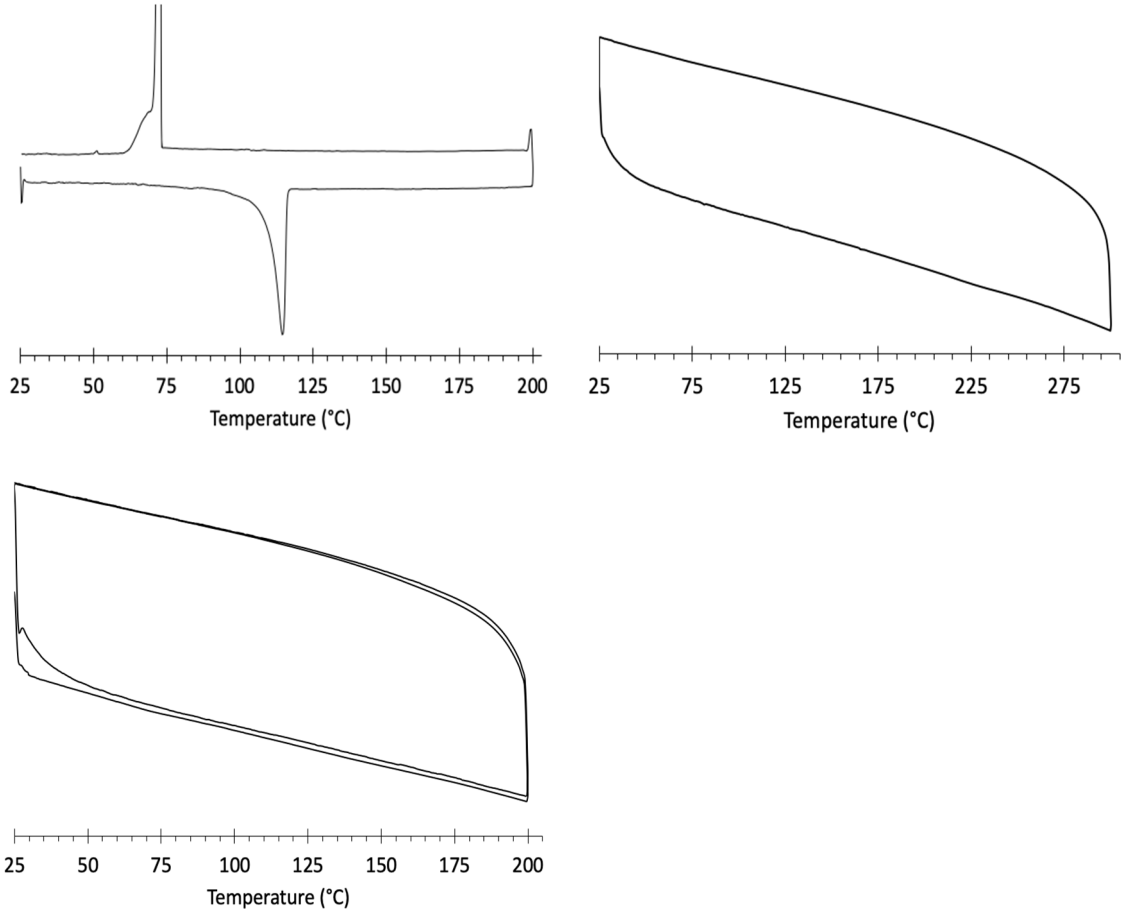

Figure S3.1 DSC profiles of $(PhCNSSN)_2$ (top left), MIL-53(Al)-*ht* (top right), and PhCNSSN@MIL-53(Al) (bottom left)

S3.2 DSC Studies on PhCNSeSeN@MIL-53(Al)

DSC studies were undertaken on PhCNSeSeN@MIL-53(Al) as well as pristine $(PhCNSeSeN)_2$ and activated MIL-53(Al). The parent radical exhibits a distinct endotherm in the region of 185 ^{o}C (Figure S3.2) but the pristine MIL-53(Al) framework and the PhCNSSN@MIL-53(Al) inclusion complex show no clear exotherm or endotherm in this temperature range.

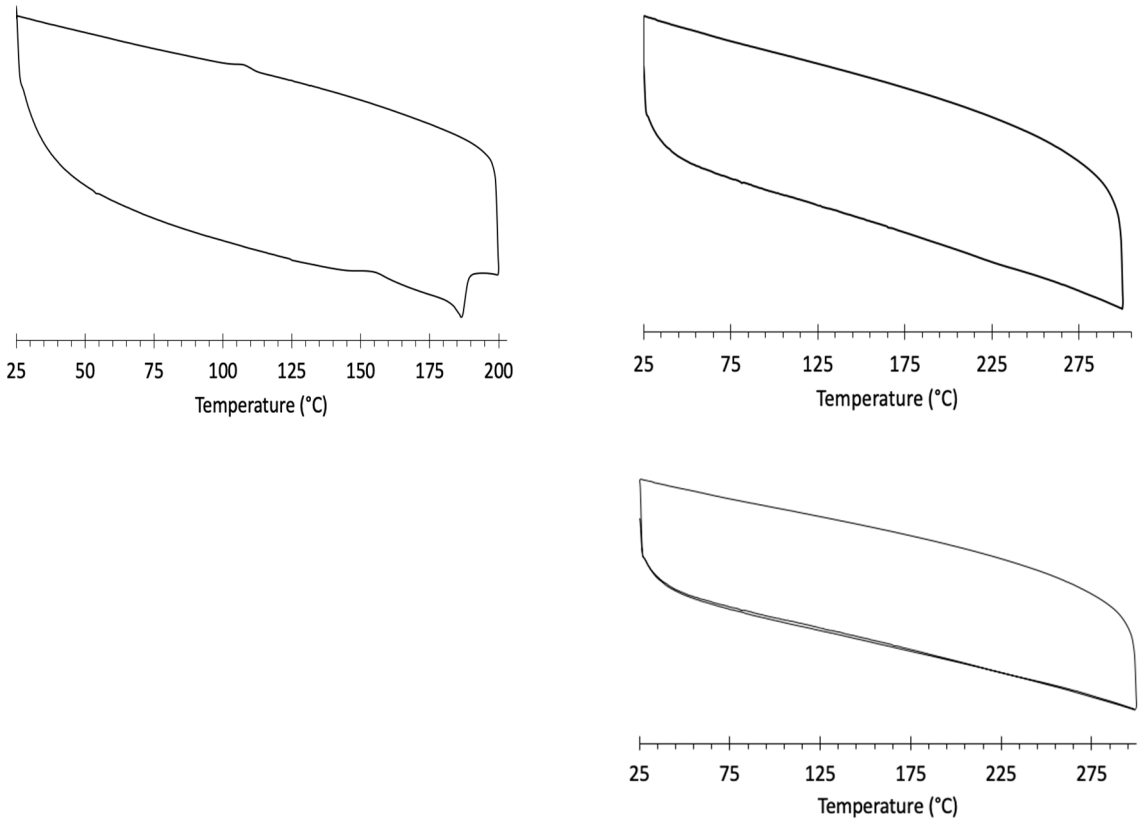

Figure S3.2 DSC profiles of $(PhCNSeSeN)_2$ (top), MIL-53(Al)-*ht* (bottom left), and PhCNSeSeN@MIL-53(Al) (bottom right)

S3.3 TGA comparison of $(PhCNSSN)_2$, MIL-53(Al) and PhCNSSN@MIL-53(Al)

A comparison of the TGA traces for $(PhCNSSN)_2$, MIL-53(Al) and PhCNSSN@MIL-53(Al) is shown in Figure S3.3. The MIL-53(Al) framework is stable, showing essentially no mass loss up to 500 ^oC, while $(PhCNSSN)_2$ commences mass loss around 60 ^oC (through sublimation) which becomes more pronounced in the 140 – 220 ^oC region. The change in shape of the profile for $(PhCNSSN)_2$ above 240 ^oC maybe indicates the onset of a decomposition process at elevated temperatures competing with sublimation. Above 300 ^oC $(PhCNSSN)_2$ reveals a near static residual 8% mass indicative of a less volatile material formed through a thermal degradation process. In contrast PhCNSSN@MIL-53(Al) commences mass loss around 140 ^oC, with a total 21% mass loss observed by 500 ^oC (corresponding to ca. 0.3 per MIL-53(Al) unit). Since the weight loss had not formed a plateau by 500 ^oC, it suggests a minimum loading of 0.3 PhCNSSN per MIL-53(Al), in good agreement with that estimated from elemental analysis data.

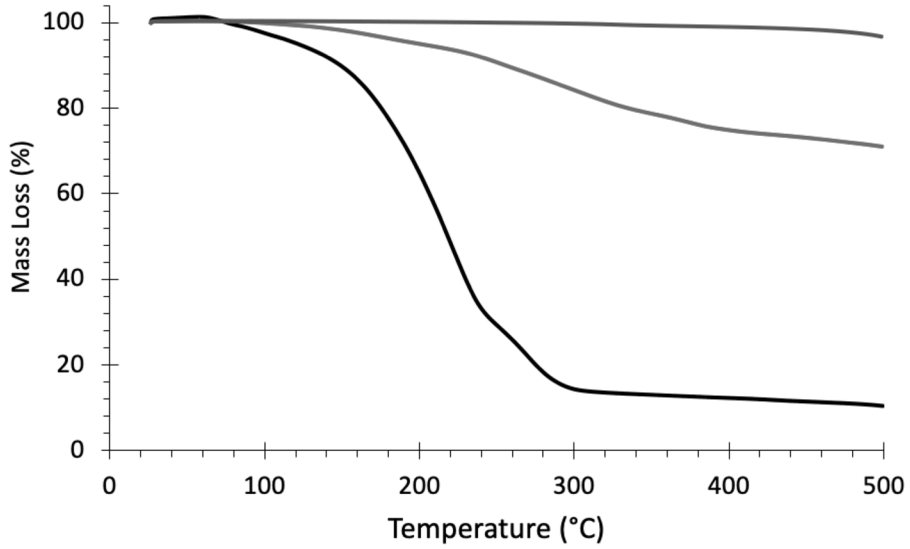

Figure S3.3 TGA profile for MIL-53(Al) (grey), PhCNSSN@MIL-53(Al) (red), and $(PhCNSSN)_2$ (black).

S3.4 Comparison of $(PhCNSeSeN)_2$, MIL-53(Al) and PhCNSeSeN@MIL-53(Al)

The thermal stability of $(PhCNSeSeN)_2$, MIL-53(Al) and PhCNSeSeN@MIL-53(Al) are presented in Figure S3.4. $(PhCNSeSeN)_2$ is less volatile than $(PhCNSSN)_2$ (section S3.1), reflected in mass loss commencing abruptly at 180 ^oC. The stepped nature of the TGA trace for $(PhCNSeSeN)_2$ reflects several competing mass loss processes, suggesting some radical degradation at elevated temperatures, leading to a residual 8% mass by 500 ^oC. In contrast a 22% mass loss was observed for PhCNSeSeN@MIL-53(Al), corresponding to an approximate composition of 0.21PhCNSeSeN@MIL-53(Al). Since the weight loss had not formed a plateau by 500 ^oC, it suggests a minimum loading of 0.21 PhCNSeSeN per MIL-53(Al) unit, in good agreement with elemental analysis data.

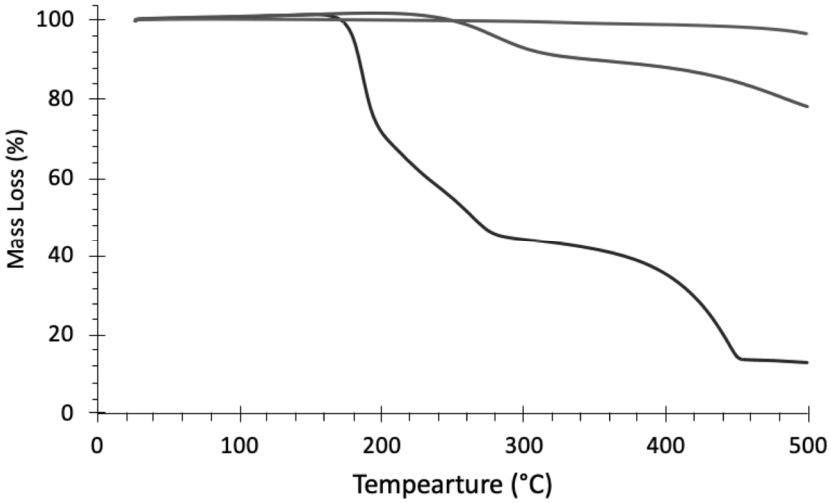

Figure S3.4 TGA profile for MIL-53(Al) (grey), PhCNSeSeN@MIL-53(Al) (purple), and $(PhCNSeSeN)_2$ (black).

S4 Mass Spectrometry

S4.1 Mass spectrometry on PhCNSSN@MIL-53(Al)

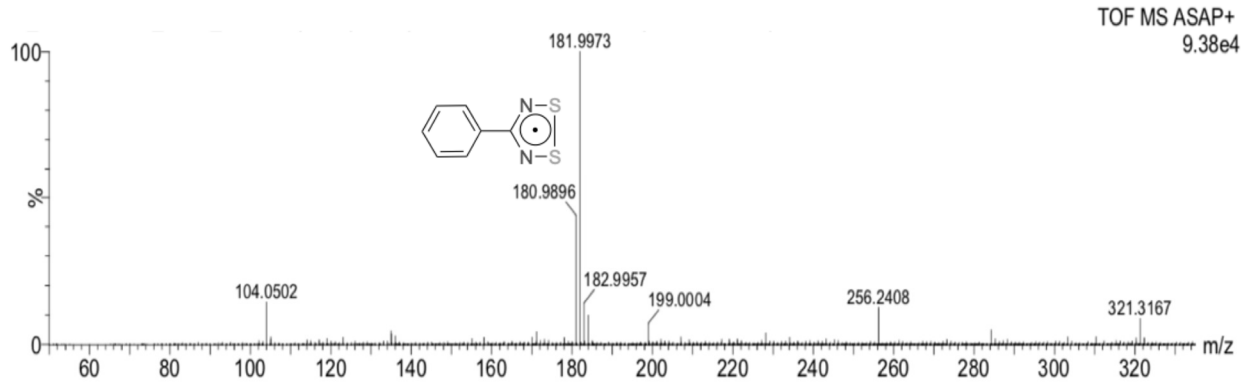

Figure S4.1 HRMS spectrum (ASAP+,200 ^{o}C) of PhDTDA@MIL-53(Al):[PhCNSSN+H] calc.181.9972

S4.2 Mass spectrometry on PhCNSeSeN@MIL-53(Al)

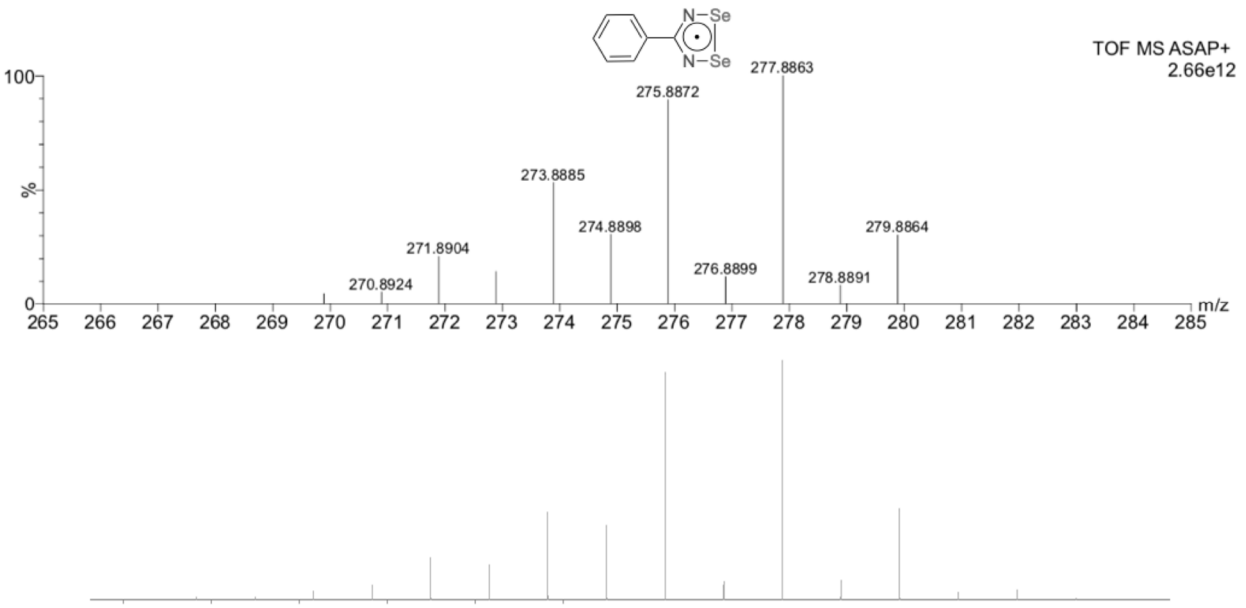

Figure S4.2 (top) HRMS spectrum (ASAP+,200 ^{o}C) of PhCNSeSeN@MIL-53(Al):[PhCNSeSeN+H] calc.277.8861; (bottom) computed isotope distribution pattern for [PhCNSeSeN+H]

S5 IR Spectroscopy

S5.1 IR Spectrum of PhCNSSN@MIL-53(Al)

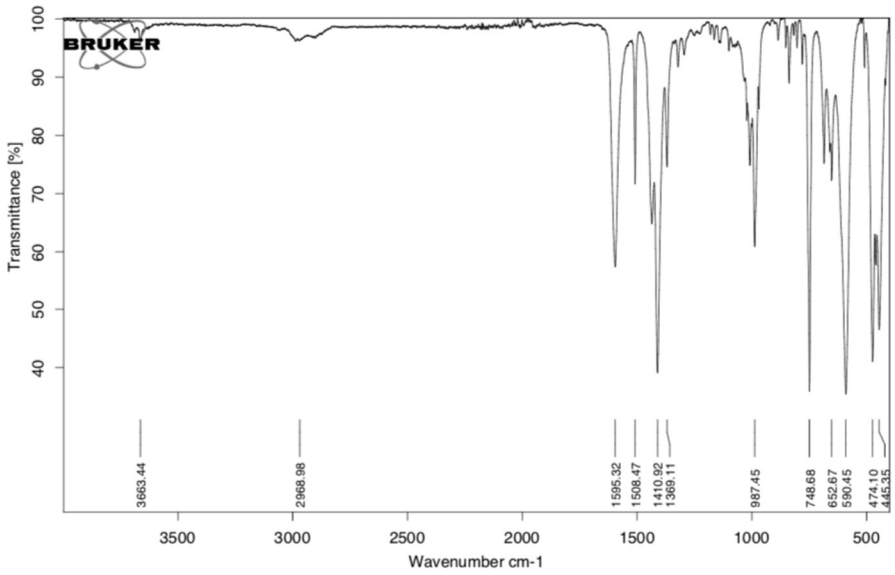

Figure S5.1 IR spectrum of PhCNSSN@MIL-53(Al)

S5.2 IR Spectrum of PhCNSeSeN@MIL-53(Al)

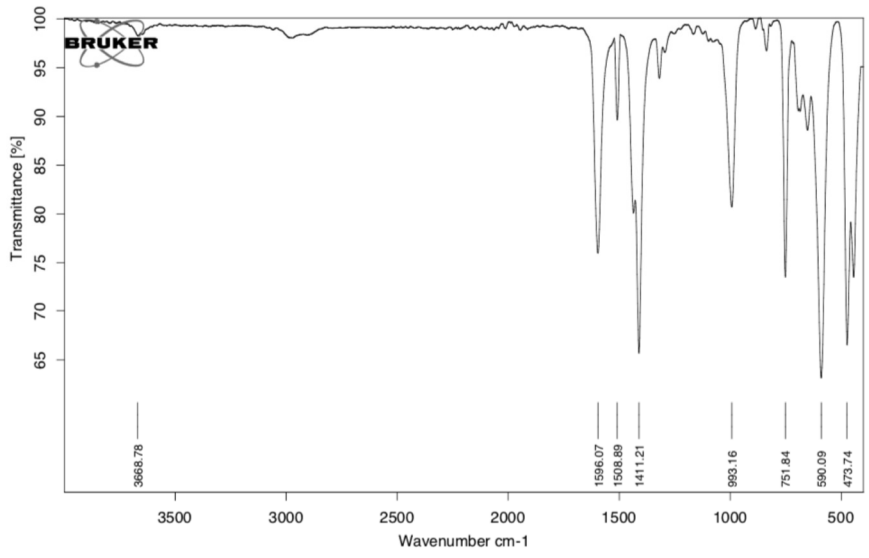

Figure S5.2 IR spectrum of PhCNSeSeN@MIL-53(Al)

S6 EPR Spectroscopy

EPR spectra were collected on a Bruker EMXplus X-band EPR spectrometer at room temperature. Simulations of anisotropic EPR spectra implemented the Fortran program PIP [1] through the PIP4WIN GUI [2]. For PhCNSeSeN the simulation comprised two components; that containing no ^{77}Se (85%) and the isotopomer containing just one ^{77}Se (14%). The isotopomer containing two ^{77}Se is calculated to be just 0.6% abundant and was neglected in the simulations. The solid state EPR spectra for PhCNSSN@MIL-53(Al) and PhCNSeSeN@MIL-53(Al) are presented in Figures S6.1 and S6.2 along with their simulations. Simulation parameters are presented in Tables S6.1 and S6.2.

[1] "PIP" M. Nilges, Ilinois EPR Research Centre, University of Illinois.
[2] "PIP4WIN v1.2" J.M. Rawson, University of Windsor.

S6.1 EPR Spectrum of PhCNSSN@MIL-53(Al)

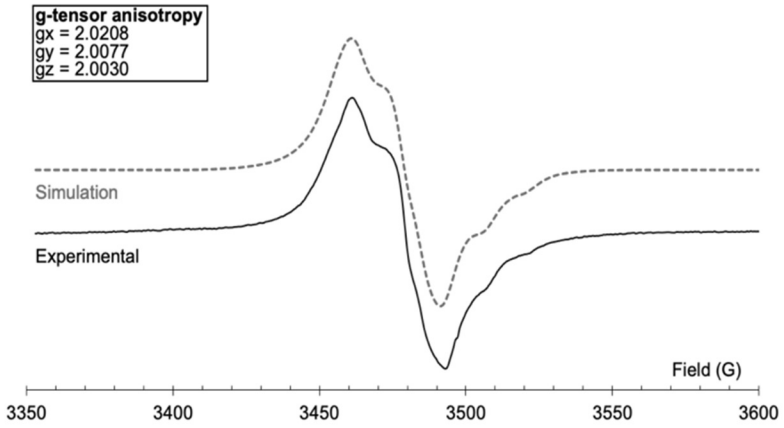

Figure S6.1 Solid state EPR spectrum of PhCNSSN@MIL-53(Al)

Component	g-factor	A_N (G)
X	2.0208	0.5
Y	2.0077	0.5
Z	2.0030	14.5
Average	2.0105	5.2

Table S6.1 EPR simulation parameters for PhCNSSN@MIL-53(Al)

S6.2 EPR Spectrum of PhCNSeSeN@MIL-53(Al)

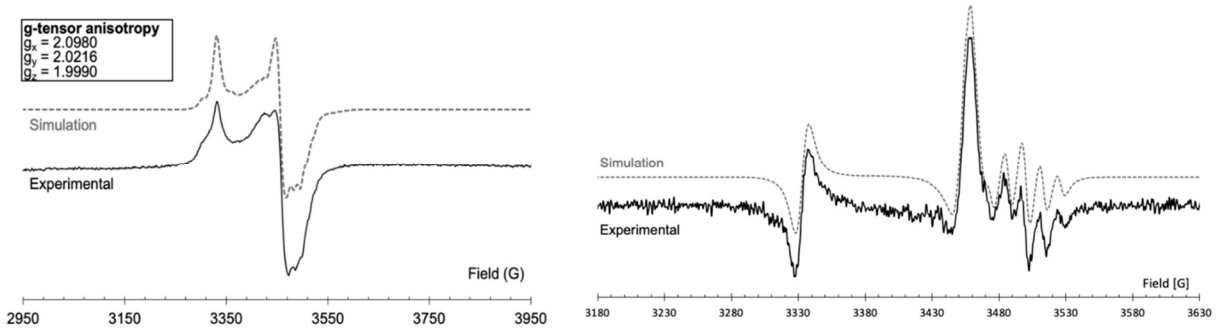

Figure S6.2 (left) First derivative solid state EPR spectrum of PhCNSeSeN@MIL-53(Al); (right) second derivative solid state EPR spectrum of PhCNSeSeN@MIL-53(Al). The dotted red lines represent the simulation using the parameters in Table S6.2.

Table S6.2 Simulation parameters for the EPR spectrum of PhCNSeSeN@MIL-53(Al)

Component	g-factor	a_N (G)	A_{Se} (G)
X	2.0980	1.3	58
Y	2.0216	1.8	56
Z	1.9990	13	130.66
Average	2.0395	5.4	81.55

S6.3 EPR Spectroscopic studies to monitor leaching of the radicals from MIL-53(Al)

Both inclusion complexes, PhCNSSN@MIL-53(Al) and PhCNSeSeN@MIL-53(Al), were suspended in dry THF for 30 minutes. PhCNSSN exhibits a high solubility in THF whereas PhCNSeSeN has negligible solubility in this solvent. After 30 minutes, EPR spectra were recorded on both samples. For PhCNSSN@MIL-53(Al), the anisotropic EPR spectrum associated with PhCNSSN@MIL-53(Al) was replaced by an isotropic five-line pentet EPR signal, consistent with extraction of the PhCNSSN radical from the framework (Figure S6.3). Conversely PhCNSeSeN@MIL-53(Al) maintained an anisotropic EPR spectrum, closely resembling that of PhCNSeSeN@MIL-53(Al), indicating the PhCNSeSeN radical is retained within the cavity. A similar experiment was completed with dry DCM instead of THF, and identical results were observed, suggesting the selenium radical is retained within the MOF, and is not as easily displaced as its sulfur analogue.

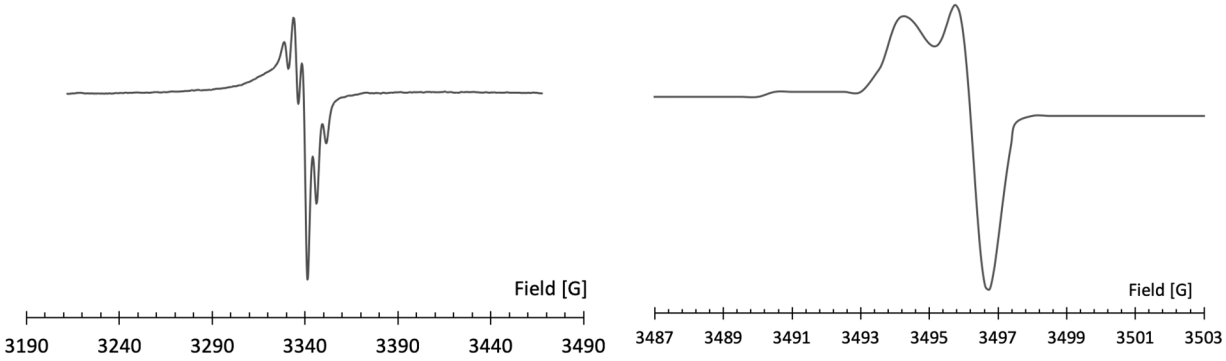

Figure S6.3 Room temperature EPR X-band spectra of (left) PhCNSSN@MIL-53(Al) and (right) PhCNSeSeN@MIL-53(Al), following suspension in dry THF for 30 minutes.

S7 SQUID Studies on Inclusion Complexes

SQUID studies were made on a sample of PhCNSSN@MIL-53(Al) (55.25 mg) and a sample of PhCNSeSeN@MIL-53(Al) (52.95 mg). Chemical compositions were estimated as 0.34PhCNSSN@MIL-53(Al) and 0.20PhCNSeSeN@MIL-53(Al) based on analytical data measured on material drawn from the same sample as that implemented for SQUID studies. Molecular weights were computed per S = ½ radical, i.e. 1 PhCNSSN:2.94 MIL-53(Al) (MW = 793 g/mol) and 1 PhCNSeSeN:5 MIL-53(Al) (MW = 1315.6 g/mol). Dc susceptibility measurements were made in a 1.0 T applied field and a diamagnetic correction applied to optimise the fit to Curie-Weiss behaviour. Both inclusion complexes obeyed Curie-Weiss behaviour (Figure S7) and values of χT substantially lower than that expected for an S = ½ paramagnet (0.375 emu·K·mol^{-1}), consistent with substantial spin-pairing (dimerization) within the channel structure. The experimental value of χT for PhCNSSN@MIL-53(Al) corresponds to just 10% of that expected for an S = ½ paramagnet whereas that for PhCNSeSeN@MIL-53(Al) corresponds to 36% of that expected for an S = ½ paramagnet.

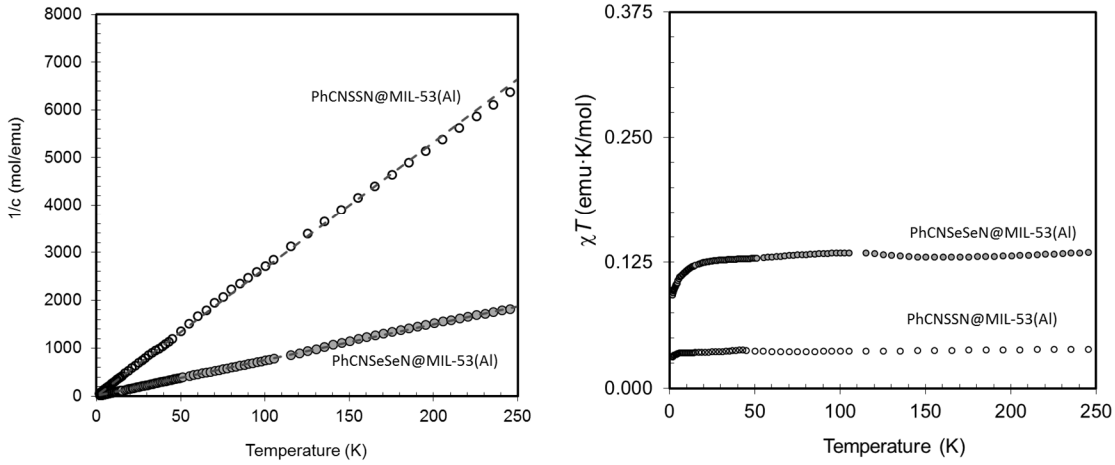

Figure S7. (left) Plots of 1/χ *vs* T for PhCNSSN@MIL-53(Al) (open circles) and PhCNSeSeN@MIL-53(Al) (grey circles) with the red dashed line reflecting the fit to Curie-Weiss behaviour (C = 0.0377 emu.K.mol^{-1}, θ = -0.7 K, R^2 = 0.9994 for PhCNSSN@MIL-53(Al) and C = 0.135 emu.K.mol^{-1}, θ = -1.8 K, R^2 = 0.9993 for PhCNSeSeN@MIL-53(Al)); (right) temperature dependence of χT.

S8. Halogenation of PhCNSSN@MIL-53(Al) and PhCNSeSeN@MIL-53(Al)

S8.1 Elemental analysis

Calc	C	H	N
0.33PhCNSSNCl@MIL-53(Al)	44.31%	2.40%	3.31%
Found	42.88%	2.81%	3.29%
0.33PhCNSSNBr@MIL-53(Al)	42.10%	2.28%	3.14%
Found	39.95%	2.34%	3.01%
0.33PhCNSSN(⅓I)@MIL-53(Al)	43.96%	2.38%	3.28%
Found	42.88%	2.71%	3.29%
0.19PhCNSeSeNCl@MIL-53(Al)	41.97%	2.25%	1.99%
Found	38.00%	2.22%	1.98%
0.19PhCNSeSeNBr@MIL-53(Al)	40.69%	2.18%	1.93%
Found	40.70%	2.15%	0.58%
0.19PhCNSeSeN(I_3)@MIL-53(Al)	33.69%	1.80%	1.60%
Found	33.91%	2.00%	1.70%

S8.2 Optical studies

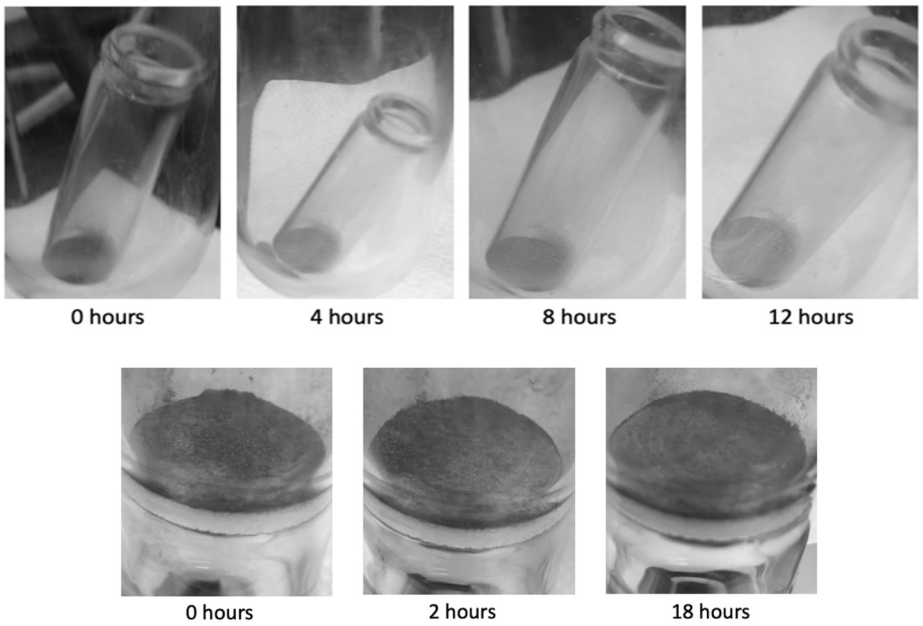

Figure S8.2 (top) Progress of chlorination of PhCNSSN@MIL-53(Al) over a 12h period at room temperature; (bottom) progress of bromination of PhCNSeSeN@MIL-53(Al) over 18h.

S8.3 PXRD studies

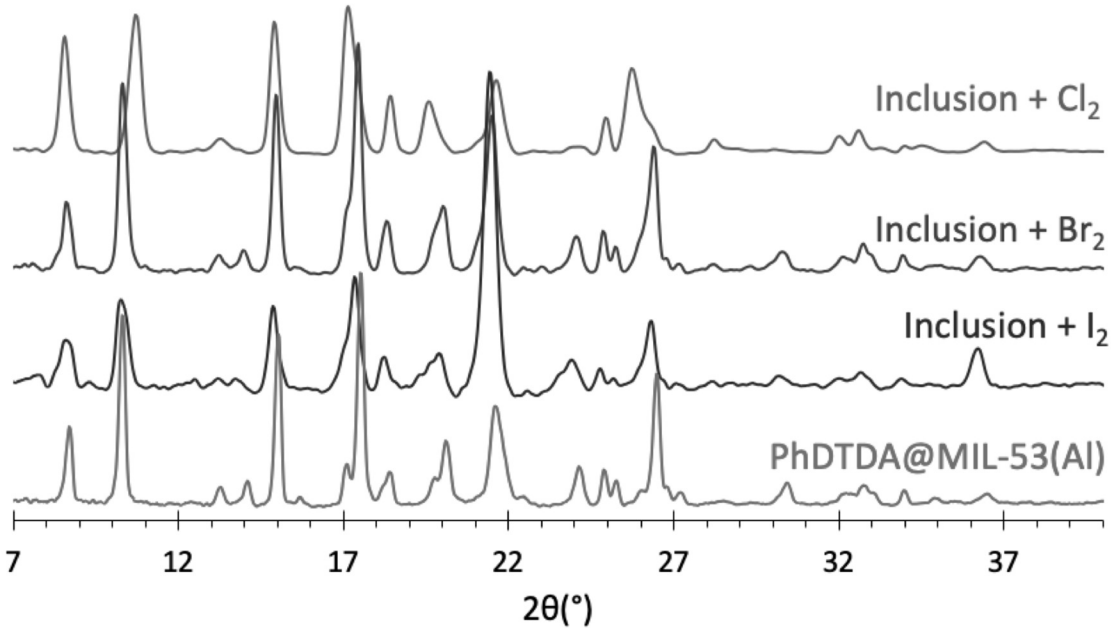

Figure S8.3 PXRD patterns of PhCNSSN@MIL-53(Al) following halogenation experiments.

S8.4 EPR Studies on iodination of PhCNSSN@MIL-53(Al) and PhCNSeSeN@MIL-53(Al)

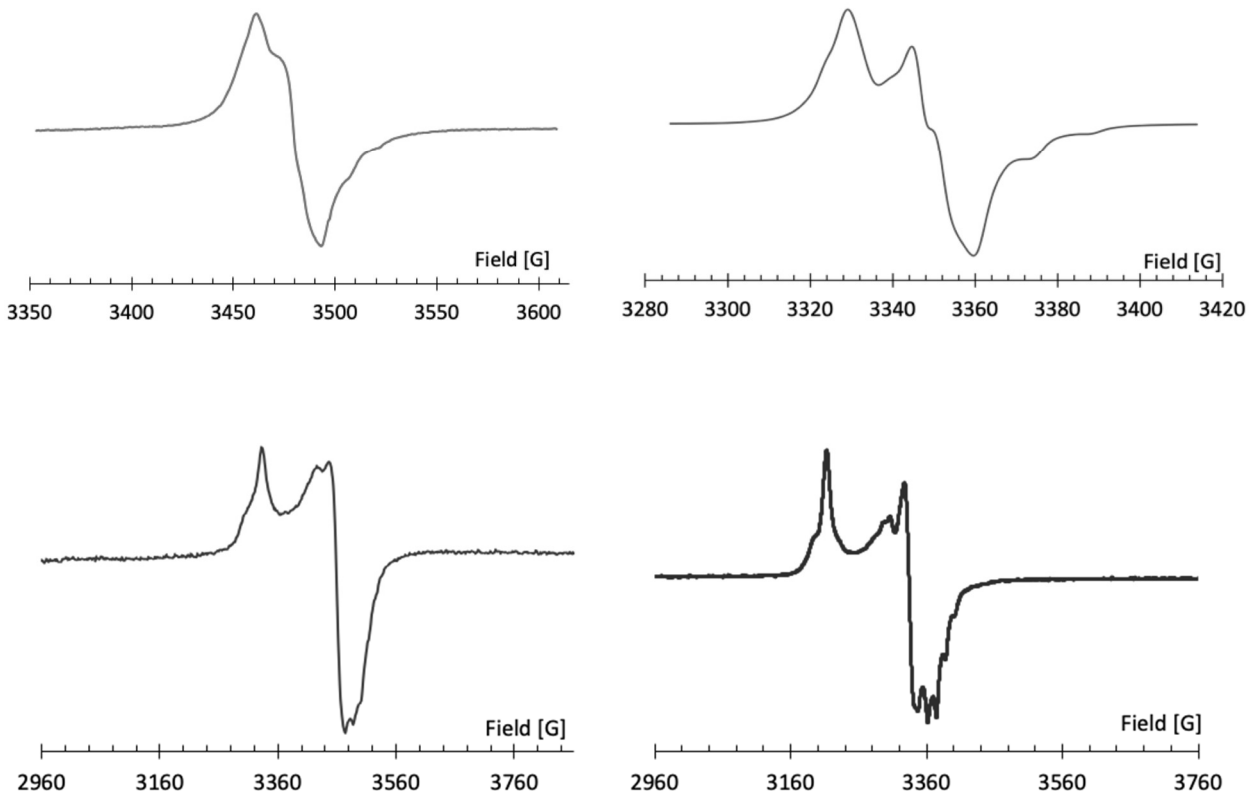

Figure S8.4 Room temperature EPR spectra of PhDTDA@MIL-53(Al) prior to iodination (top left) and following iodination (top right); PhDSDA@MIL-53(Al) prior to iodination (bottom left) and following iodination (bottom right).